Journal of Mammalian Evolution
https://doi.org/10.1007/s10914-018-9441-1

ORIGINAL PAPER

# Digital Cranial Endocasts of the Extinct Sloth *Glossotherium robustum* (Xenarthra, Mylodontidae) from the Late Pleistocene of Argentina: Description and Comparison with the Extant Sloths

Alberto Boscaini[1] · Dawid A. Iurino[2,3] · Raffaele Sardella[2,3] · German Tirao[4] · Timothy J. Gaudin[5] · François Pujos[1]



**Abstract**
The internal cranial morphology of the terrestrial sloth *Glossotherium robustum* is described here based on a neurocranium from the late Pleistocene of the Pampean region of Buenos Aires, northeastern Argentina. The first published data on the morphology of the brain cavity of this species date back to the latest nineteenth century. The novel techniques of CT scanning and digital reconstructions enable non-destructive access to the internal cranial features of both extinct and extant vertebrates, and thus improve our knowledge of anatomical features that had previously remained obscure. Therefore, we performed CT scans on the posterior half of a skull of *G. robustum* and created digital models of the endocasts and internal structures. The results reveal the morphology of the brain cavity itself, as well as the paranasal sinuses and the trajectory of several cranial nerves and blood vessels. These features have been compared with the two extant folivoran genera, the two-toed sloth *Choloepus* and the three-toed sloth *Bradypus*. For many characteristics, especially those related to the paranasal pneumaticity and the brain cavity, a closer similarity between *Glossotherium* and *Choloepus* is observed, in accordance with the most widely accepted phylogenetic scenarios. However, other features are only shared by the two extant genera, but are probably related to allometric effects and the convergence that affected the two modern lineages. This study, which represents the first exhaustive analysis of digital endocasts of a fossil sloth, reveals the importance of the application of new methodologies, such as CT scans, for elucidating the evolutionary history of this peculiar mammalian clade.

**Keywords** Extinct sloth *Glossotherium* · Endocast · Brain cavity · Cranial nerves · Paranasal sinuses · Blood vessels

✉ Alberto Boscaini
aboscaini@mendoza-conicet.gob.ar; alberto.boscaini@gmail.com

[1] Instituto Argentino de Nivología, Glaciología y Ciencias Ambientales (IANIGLA), CCT-CONICET-Mendoza, Avda. Ruiz Leal s/n, Parque Gral. San Martín, 5500 Mendoza, Argentina

[2] Dipartimento di Scienze della Terra, Sapienza Università di Roma, Piazzale A. Moro 5, 00185 Rome, Italy

[3] PaleoFactory, Sapienza Università di Roma, Piazzale A. Moro 5, 00185 Rome, Italy

[4] IFEG (CONICET), Facultad de Matemática, Astronomía y Física, Universidad Nacional de Córdoba, Haya de la Torre y Medina Allende, X5000HUA Córdoba, Argentina

[5] Department of Biology, Geology, and Environmental Sciences, University of Tennessee at Chattanooga, 615 McCallie Ave, Chattanooga, TN 37403-2598, USA

## Introduction

Xenarthrans are among the most peculiar mammals of the South American endemic Cenozoic fauna (Simpson 1980). South America's period of isolation began in the late Paleocene, when its land connection with Antarctica was lost (Reguero et al. 2014), and finished with the formation of the Panamanian isthmus and connection with North America, around 2.8 Ma (Woodburne 2010). During the Tertiary period, only some "sweepstakes" or "island hopping" interchanges took place, such as the middle Eocene and early Oligocene immigration of rodents and primates, respectively, from Africa (Antoine et al. 2012). Other migrations before the G.A.B.I. (Great American Biotic Interchange) were observed in the early Miocene (about 18 Ma, through the West Indies) and in the late Miocene (about 7 Ma, probably through Central

Published online: 07 June 2018

America) (MacPhee and Iturralde-Vinent 1994, 1995; Pascual 2006; McDonald and De Iuliis 2008).

The fossil record of xenarthrans begins soon after the separation of South America and Antarctica, in the early Eocene, with armadillos from the Itaboraí fauna (Itaboraian SALMA [South American Land Mammal Ages], southeastern Brazil; Bergqvist et al. 2004; Gelfo et al. 2009) and continues throughout the Cenozoic, with representatives of all three major groups of Xenarthra persisting to the present: Cingulata (armadillos; also including extinct glyptodonts and pampatheres), Vermilingua (anteaters), and Folivora (sloths) (e.g., Engelmann 1985; Gaudin 2004). According to Gaudin and Croft (2015), the oldest representatives of these clades date back to the early Eocene, the early Miocene, and the late Eocene, respectively.

Folivora (=Tardigrada = Phyllophaga; Delsuc et al. 2001; Fariña and Vizcaíno 2003) includes all extant and extinct sloths, the diversity of which is considerably more pronounced in the fossil record than in the present day (more than 90 fossil genera against the only two surviving ones, *Bradypus* and *Choloepus*; McKenna and Bell 1997). The diphyletic origin of the two extant sloth genera is henceforth accepted (e.g., Gaudin 2004; Pujos et al. 2017): recent phylogenetic analysis based on osteological characters (e.g., Gaudin 1995, 2004) consider *Bradypus* the sole representative of Bradypodidae and the sister taxon of the other sloths, and *Choloepus* as the only living member of Megalonychidae. The other three extinct sloth clades are the Nothrotheriidae, the Megatheriidae, and the Mylodontidae (e.g., Engelmann 1985; Gaudin 2004; McDonald and De Iuliis 2008), but their relationships are still debated (e.g., Gaudin 2004; Slater et al. 2016). The successful radiations of mylodontid and megalonychid sloths, the first to appear in the fossil record, took place in the late Oligocene, as documented by the numerous sloth skeletal remains referable to the Deseadan SALMA, and persisted until the late Pleistocene/Holocene periods (Gaudin and Croft 2015; Slater et al. 2016; Pujos et al. 2017).

Among the Mylodontidae, *Glossotherium* (literally "Tongue Beast") was historically the first genus described (Owen 1839). The name was inspired by the exceptional size of the stylohyal fossa and the hypoglossal foramen, two basicranial structures directly linked to the tongue (the first in providing a synovial attachment for the stylohyal bone, part of the massive hyoid apparatus (Pérez et al. 2010) that served for attachment of tongue muscles, and the second for passage of the hypoglossal nerve [XII] that innervates the tongue muscle; Owen 1839). The robust tongue, coupled with the action of the lips, facilitated food intake in this extinct sloth, the diet of which was mainly comprised of grass and herbaceous plants (Bargo et al. 2006b; Bargo and Vizcaíno 2008). *Glossotherium* has, in fact, often been associated with open and temperate habitats (Czerwonogora et al. 2011) and commonly recovered in Pleistocene localities from austral areas of the South American continent (e.g., Pitana et al. 2013; Varela and Fariña 2016).

The taxonomic history of *Glossotherium* is confusing (Mones 1986, listed 32 specific and sub-specific names), and highly convoluted (for a resume, see Esteban 1996; Fernicola et al. 2009; McAfee 2009; De Iuliis et al. 2017). A recent detailed systematic revision performed by Esteban (1996) recognized only two *Glossotherium* species: *G. robustum* and *G. chapadmalensis*. McAfee (2009) shared the same opinion, even though he allowed for the possibility that *G. chapadmalensis* belonged to another genus (i.e., *Eumylodon*), following the original description of Kraglievich (1925). Recently, Pitana et al. (2013) also considered valid *G. lettsomi* from the Pleistocene of Argentina, Chile, and Uruguay (Ameghino 1889; Pitana et al. 2013 and references therein), *G. wegneri* from the Pleistocene of Brazil and Ecuador (Hoffstetter 1952; Simpson and Paula-Couto 1981), *G. tropicorum* from the late Pleistocene of Ecuador and Venezuela (Hoffstetter 1952; Bocquentin 1979), and an indeterminate *Glossotherium* species, widely distributed into the intertropical latitudes of the South American continent. In the most recently updated listing of extant and extinct sloths, Pujos et al. (2017) ascribed four species under the genus *Glossotherium*: *G. robustum*, *G. tarijensis*, and *G. tropicorum*, and the intertropical *Glossotherium* species (currently under study by Cartelle and colleagues). Recently, De Iuliis et al. (2017) performed a comprehensive revision of *G. tropicorum* from the late Pleistocene of Ecuador and Peru.

Considering this context, a detailed and comprehensive revision of the genus is necessary. However, for the purposes of the present study, the target taxon *G. robustum*, the type species of the genus *Glossotherium,* remains indisputably recognized as a valid taxon. It is also the best known and geographically most widely distributed species of *Glossotherium* in South America (McAfee 2009; Pitana et al. 2013).

In recent years, diverse studies have focused on *G. robustum*, increasing knowledge of several aspects of its paleobiology, such as its body mass (Christiansen and Fariña 2003), digging abilities (Bargo et al. 2000; Vizcaíno et al. 2001), dietary preferences and food intake (Bargo et al. 2006a, b; Bargo and Vizcaíno 2008; Pérez et al. 2010; Czerwonogora et al. 2011), and hearing capabilities (Blanco and Rinderknecht 2008, 2012). Furthermore, its paleobiogeography has been analyzed in detail (i.e., Varela and Fariña 2016), and several diagnostic anatomical features have been clarified (McAfee 2009; Pitana et al. 2013).

Nevertheless, studies on the internal cranial anatomy of *Glossotherium* have been long neglected and, to date, digital endocast reconstructions are unknown in this or any other fossil sloth. Indeed, studies of the encephalic cavity of fossil sloths and the brains of living sloths, date back to the nineteenth century (e.g., Gervais 1869; Elliot-Smith 1898). Additional descriptive works on the anatomy of the internal encephalic cavitiy of extinct sloths were conducted by Colette Dechaseaux in the mid-twentieth century (Dechaseaux 1958, 1962a, b, 1971). This

author described and figured many fossil genera, such as *Glossotherium*, *Hapalops, Lestodon, Megatherium*, and *Oreomylodon*, based on plaster casts of the brain cavity, the most commonly employed technique at that time [(Dechaseaux 1958, 1962a, b, 1971; regarding the latter genus, the revisions of St-André et al. (2010) and Antoine et al. (2017) are followed here, in recognizing *Oreomylodon* as a separate genus, rather than a subgenus of *Glossotherium*, as in Hoffstetter (1952)]. Following the same methodology, Dozo (1987, 1994) studied the middle Miocene forms *Eucholoeops* and *Hapalops* from Santa Cruz Province.

To our knowledge, only limited information is available on the paranasal pneumaticity in xenarthrans, and exhaustive studies are restricted to two representatives of Cingulata: the extant genus *Dasypus* (Billet et al. 2017) and the peculiar extinct glyptodont *Neosclerocalyptus* (Fernicola et al. 2012). The most detailed study on sinuses in anteaters is that of Storch and Habersetzer (1991). The morphology of the frontal sinuses in extant sloths was briefly mentioned by Moore (1981), Langworthy (1935), and Goffart (1971) for *Choloepus,* and illustrated for *Bradypus* and *Choloepus* by Naples (1982) using radiographs. In extinct sloths, some annotations on the development of frontal and sphenoidal sinuses are mentioned in Dechaseaux (1971) and McDonald et al. (2013), respectively, concerning the mylodontid *Oreomylodon* and the megalonychid *Megistonyx*. Pterygoid and epitympanic sinuses in the squamosal are described by Patterson et al. (1992) for several extinct sloths. These authors noted the remarkable pneumatization of the skull in the large Pleistocene Antillean sloth *Megalocnus*. Inflation of the pterygoid and frontal bones was codified as characters 137 and 174 by Gaudin (2004: appendix 2).

The aims of the present work are to provide the first digital reconstruction of a fossil sloth's endocranial casts, with preliminary discussions on their possible phylogenetic, allometric, and functional value. Particular emphasis is placed on the brain cavity, along with the cranial nerves, the intracranial vasculature, and the pneumatized structures of the cranium, to provide an anatomical characterization of the main features, alongside comprehensive comparisons with the available literature (Gervais 1869; Dechaseaux 1958, 1962a, b, 1971; Dozo 1987, 1994). However, due to a paucity of data on these features in extinct sloths, the structures in *Glossotherium* will be compared with their homologues in the extant *Bradypus* and *Choloepus*.

## Materials and Methods

The neurocranium of *Glossotherium robustum* (MACN Pv 13553; see below for institutional abbreviations) was recovered in 1933 near the city of Tandil (Buenos Aires Province, Argentina). It was scanned using the General Electric Lightspeed CT scanner in FUESMEN institute. The scanning resulted in 839 slices with a slice thickness of 0.62 mm. The comparative sample is based on two complete skulls of the extant sloths *Choloepus hoffmanni* (AMNH 30765) and *Bradypus variegatus* (AMNH 95105). Their CT images were downloaded from the Digital Morphology library (www.digimorph.org). *Choloepus hoffmanni* (AMNH 30765) was scanned with a slice thickness of 0.241 mm, producing a total of 441 slices, whereas the slice thickness for *B. variegatus* (AMNH 95105) was 0.197 mm, yielding a total of 369 slices. The image segmentation process for the three specimens was performed using the digital tools from OsiriX v.5.6 32-bit and Materialise Mimics v.17. The 3D models of skulls, brains, frontal sinuses, and inner ears, exported from Mimics as ".PLY" files, were converted to ".OBJ" format and imported into ZBrush 4R6 for the rendering process. Because of the presence of infilled sediment in different cranial cavities of MACN Pv 13553, the segmentation process was carried out manually, slice-by-slice.

All the specimens considered in this study are adults, as shown by the complete fusion of cranial sutures. Analyzing taxa of comparable developmental stages helps to avoid variability due to ontogenetic development.

Identification of endocranial structures was based on previous descriptions of sloth endocasts (e.g., Dechaseaux 1958, 1962a, b, 1971; Dozo 1987, 1994), as well as classic manuals on the anatomy of domestic mammals (Evans 1993; Barone and Bortolami 2004; Constantinescu and Schaller 2012) and extant xenarthrans (Hyrtl 1854; Tandler 1901; Bugge 1979).

All data generated or analyzed during the current study are available from the corresponding author on reasonable request.

### Institutional Abbreviations

**A**, Gervais Collection, Laboratoire d'Anatomie Comparée du Muséum National d'Historie Naturelle, Paris, France; **AMNH**, American Museum of Natural History, New York, USA; **FUESMEN**, Fundación Escuela de Medicina Nuclear, Mendoza, Argentina; **MACN Pv**, Colección de Paleontología de Vertebrados, Museo Argentino de Ciencias Naturales "Bernardino Rivadavia," Buenos Aires, Argentina.

## Systematic Paleontology

Superorder XENARTHRA Cope, 1889
Order PILOSA Flower, 1883
Suborder FOLIVORA Delsuc et al., 2001
Family MYLODONTIDAE Gill, 1872
Subfamily MYLODONTINAE Gill, 1872
Genus ***Glossotherium*** Owen, 1839
***Glossotherium robustum*** (Owen, 1842)

**Referred Material** MACN Pv 13553, neurocranium (Fig. 1). This specimen consists of the posterior portion of a skull of *G. robustum*. The cranial roof and the anterior half of the skull are lacking, exposing the sinuses that comprise the pneumatized structures around the braincase (Fig. 1). The zygomatic processes of both squamosals are also broken at their bases. The external aspect of this specimen and the anatomy of the inner ear have been recently described in detail by Boscaini et al. (2018).

**Stratigraphic and Geographic Occurrence** Upper Pampean Formation (late Pleistocene), Tandil, Buenos Aires Province, Argentina.

## Description and Comparison

### Brain Endocast

The 3D model of the brain digital endocast of *Glossotherium* is almost complete, with the exception of the dorsal portion of the left olfactory bulb, which was impossible to reconstruct due to the lack of bony material (Fig. 2a-d). In general, the external surface is well preserved and the pattern of convolutions and the majority of blood vessels and nerves are recognizable. As expected, the brain of *Glossotherium* was considerably larger than that of the extant forms *Choloepus* and *Bradypus*, both in terms of linear measures and volume (Fig. 2). At first glance, the patterns of convolutions in the cerebral hemisphere of these three genera are different, with *Glossotherium* showing a higher level of complexity than the endocasts of the two extant taxa (Fig. 2).

However, the seemingly higher degree of complexity is not related to an increase in number of the convolutions, but to the presence of surface irregularities. These latter are in fact small recesses and protrusions of irregular shape and limited extent, not compatible with the morphology of convolutions mentioned in the literature (e.g., Barone and Bortolami 2004). A similar high degree of complexity is observed in other extinct giant sloth genera such as *Lestodon*, *Megatherium*, *Mylodon*, *Oreomylodon*, and *Scelidotherium* (Gervais 1869; Dechaseaux 1958, 1962a, b, 1971), and to a lesser extent in the small-sized extinct early sloths *Hapalops* and *Eucholoeops* (Dozo 1987, 1994).

In *Glossotherium*, the cerebrum is globular. The cerebral hemispheres arch strongly dorsally, and are separated by a very deep longitudinal fissure (Fig. 2a-d). In dorsal view the fissure is especially deep and wide anteriorly, imparting a peculiar "walnut kernel" shape to the brain. In *Choloepus* and *Bradypus*, the hemispheres are less arched and the longitudinal fissure less prominent than in *Glossotherium* (Fig. 2e-l). The morphology of the extant sloths more closely resembles that of *Hapalops* and *Eucholoeops* (Dozo 1987, 1994).

In dorsal view (Fig. 2a, e, i), the symmetric convolutions are represented mainly by the lateral and suprasylvian gyri, arranged similarly anteroposteriorly in *Glossotherium*, *Choloepus*, and *Bradypus*. The occipital gyri are oriented mediolaterally, emphasizing the transverse fissure that separates the telencephalon from the cerebellum. The entolateral sulcus, which divides the lateral gyrus anteroposteriorly into medial and lateral portions, is a feature shared only by *Glossotherium* and *Choloepus*. It is absent in *Bradypus* (Fig. 2a, e, i).

The dorsal surface of the telencephalon of *Lestodon*, *Megatherium*, *Mylodon*, *Oreomylodon*, *Scelidotherium* (Gervais 1869; Dechaseaux 1958, 1962a, b, 1971), and the

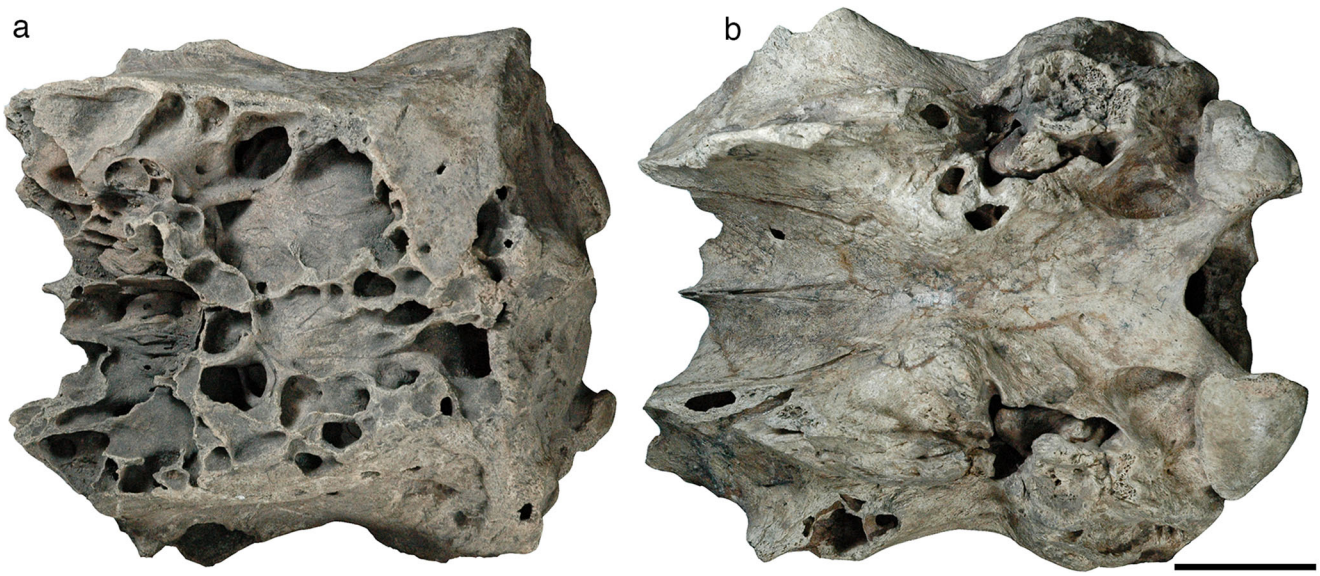


**Fig. 1** Posterior portion of the cranium of *Glossotherium robustum* (MACN Pv 13553) in dorsal (**a**) and ventral (**b**) views. Scale bar equals 5 cm

*Glossotherium* specimen figured in Dechaseaux (A10.263; 1958, 1971) is extremely similar to that of *Glossotherium* MACN Pv 13553. It comprises two globose hemispheres divided by a deep longitudinal fissure. The well-developed suprasylvian gyri are always present in these fossil genera. A deep entolateral sulcus is visible in A10.263 of *Glossotherium* (Dechaseaux 1958, 1971) and also in *Lestodon*, *Megatherium*, *Mylodon*, *Oreomylodon*, and *Scelidotherium* (Gervais 1869; Dechaseaux 1958, 1962a, 1971), whereas it seems to be absent in *Hapalops* and *Eucholoeops* (Dozo 1987, 1994).

In *Glossotherium*, *Oreomylodon*, *Lestodon*, and *Megatherium*, the entire dorsal brain surface is strongly arched and the anterior portion is very wide, bulging mediolaterally (Gervais 1869; Dechaseaux 1958, 1962a, b, 1971). However, the width of the *Megatherium* brain (Gervais 1869) strongly decreases along the pseudosylvian sulci, in contrast to the condition observed in the mylodontids mentioned above (Gervais 1869; Dechaseaux 1958, 1962a, 1971). In all these genera (including *Megatherium*), the large olfactory gyrus is delimited by a deep rhinal fissure, which is curved dorsally, its apex approaching the nearly vertical pseudosylvian sulcus (Fig. 2c; Dechaseaux 1958, 1962a, b, 1971). A well-developed pyriform lobe is delimited by the posterior margin of the rhinal fissure in *Glossotherium* (Fig. 2c) and *Oreomylodon* (Dechaseaux 1971: fig. 13) as well as in both the extant taxa (Fig. 2g, k). This fissure is generally used as an indication of the ventral limit of the neocortex, which is considered the newest portion of the cerebral hemisphere in mammals (Jerison 1991).

The olfactory bulbs of *Glossotherium* are prominent and extend strongly dorsally, with a wide and flat anterior surface covered by the ramifications of the olfactory nerve (I) (Fig. 2a-d). In anterior view, these bulbs appear "teardrop-shaped" with the dorsal part wider than the ventral one (Fig. 2d). Both bulbs are flanked by two large symmetrical blood vessels and some additional tiny vessels, which make the architecture of the olfactory bulbs in *Glossotherium* very similar to that observed in other terrestrial sloths such as *Oreomylodon* (Dechaseaux 1971). Unfortunately, a detailed comparison with the olfactory bulbs of *G. robustum* A10.263 (Dechaseaux 1958, 1971) is not possible, due to the quality of the cast of the latter. However, based on what is preserved, the morphology of the whole brain would seem to be almost identical in the two *Glossotherium* specimens.

The olfactory bulbs of *Choloepus* and *Bradypus* differ in shape. In *Choloepus*, the olfactory bulbs are well separated and their outline is rectangular in dorsal view (Fig. 2e). In lateral view, the ventral surface (bearing the ramifications of the olfactory nerve) is inclined anterodorsally (Fig. 2g), but the dorsal edge is horizontal, in contrast to the inclined orientation present in *Glossotherium*. The olfactory bulbs are reniform in anterior view, unlike the teardrop-shaped bulbs in *Glossotherium* (Fig. 2h). On the other hand, the olfactory bulbs in *Bradypus* are situated closer together. They are anteroposteriorly elongated and triangular in outline in lateral view, its margins converging to form a distinct point anteriorly, and with a horizontal dorsal edge like that of *Choloepus* (Fig. 2i). A similar condition is also observed in *Hapalops* (Dozo 1987) and *Eucholoeops* (Dozo 1994). Moreover, in anterior view, the dorsoventral height of the olfactory bulbs is greater than the transverse width in *Glossotherium* and *Choloepus* (Fig. 2d, h), whereas the opposite is observed in *Bradypus* (Fig. 2l). The general shape of the olfactory bulbs in *Glossotherium* is more similar to *Choloepus* than to *Bradypus, Hapalops*, or *Eucholoeops*.

The cerebellum of *Oreomylodon*, *Lestodon*, *Mylodon*, *Scelidotherium*, *Megatherium*, and especially *Glossotherium* is large with both cerebellar hemispheres laterally expanded (Fig. 2a, c; Gervais 1869; Dechaseaux 1958, 1962a, 1971). In these taxa, the cerebellum is sub-triangular in dorsal view with the apex formed by the posterior portion of the vermis. The latter structure is well delineated (Fig. 2a; Gervais 1869; Dechaseaux 1958, 1962a, 1971). Along the transverse fissure of all these genera (with the exception of *Scelidotherium* and *Megatherium*), the cerebellum is as wide as the posterior portion of the cerebral hemisphere (Fig. 2a). The paraflocculus is the lateral expansion of the cerebellum that is housed in the subarcuate fossa of the petrosal bone (Dechaseaux 1971; Macrini et al. 2007a, b). In *Glossotherium* MACN Pv 13553, the bulge that comprises the paraflocculus is clearly recognizable on the surface of the endocast (Fig. 2c), as it is in the endocasts of *Oreomylodon* and *Glossotherium* figured in Dechaseaux (1971). In both extant forms, the cerebellum is roughly oval in shape with the maximal width always less than that of the telencephalon (Fig. 2e, i). The lateral cerebellar hemispheres have rounded and smooth surfaces. The vermis is well developed in *Choloepus,* whereas it leaves no distinctive impression on the endocast surface of *Bradypus* (Fig. 2e, i). The parafloccular areas are poorly marked in the extant sloths, and are located just dorsal to the jugular foramen (Fig. 2g, k), as in *Glossotherium* and *Oreomylodon* (Dechaseaux 1971).

## Cranial Nerves

In *Glossotherium*, the emergence of the cranial nerves is visible in ventral, lateral, and anterior views (Fig. 2), and has been identified on the basis of Dechaseaux (1971) and Gaudin et al. (2015).

The anteriormost nerve leaving the encephalic cavity corresponds to the optic nerve (II), which extends through the optic foramen (Fig. 2b). The optic foramen opens into the sphenorbital fissure in all the observed specimens of *Glossotherium*, *Choloepus*, and *Bradypus*. The confluence of the optic foramen and the sphenorbital fissure is located anterior to the olfactory bulbs in *Glossotherium* (Fig. 2b, c),

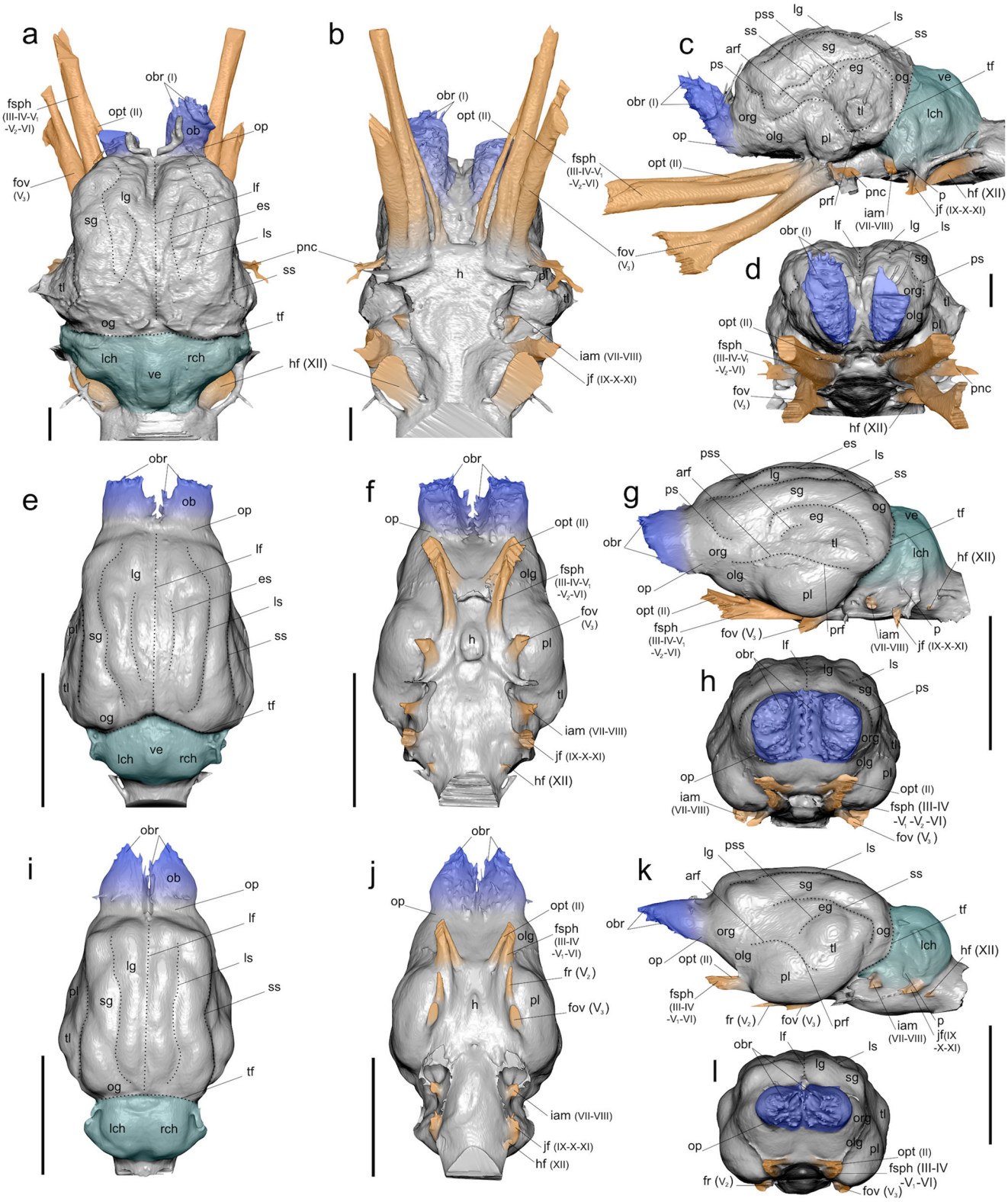


whereas it is posteriorly located in *Choloepus* (Fig. 2f, g) and *Bradypus* (Fig. 2j, k). In all the sloths, the optic foramen and the sphenorbital fissure share a common external aperture in lateral view (Gaudin 2004).

The sphenorbital fissure transmits several nerves (i.e., III-IV-$V_1$-$V_2$-VI) and is, therefore, the largest foramen in all the observed specimens. In *Glossotherium* MACN Pv 13553 (Fig. 2b-d) and *Choloepus* AMNH 30765 (Fig. 2f-h), both

◀ ◀ **Fig. 2** Brain endocasts of *Glossotherium* (MACN Pv 13553) (**a-d**), *Choloepus* (AMNH 30765) (**e-h**), and *Bradypus* (AMNH 95105) (**i-l**), in dorsal (**a**, **e**, **i**), ventral (**b**, **f**, **j**), lateral (**c**, **g**, **k**), and anterior (**d**, **h**, **l**) views. Abbreviations: arf, anterior rhinal fissure; eg, ectosylvian gyrus; es, entolateral sulcus; fov, foramen ovale; fr, foramen rotundum; fsph, sphenorbital fissure; h, hypophysis; hf, hypoglossal foramen; iam, internal acoustic meatus; jf, jugular foramen; lch, left cerebellar hemisphere; lf, longitudinal fissure; lg, lateral gyrus; ls, lateral sulcus; ob, olfactory bulb; obr, olfactory bulb ramifications; og, occipital gyrus; olg, olfactory gyrus; op, olfactory peduncle; opt, optic foramen; org, orbital gyrus; p, paraflocculus; pl, pyriform lobe; pnc, petrosal nerve complex; prf, posterior rhinal fissure; ps, presylvian sulcus; pss, pseudosylvian sulcus; rch, right cerebellar hemisphere; sg, suprasylvian gyrus; ss, suprasylvian sulcus; tf, transverse fissure; tl, temporal lobe; ve, vermis. Colors indicate: grey, cerebrum; blue, olfactory bulbs; turquoise, cerebellum; orange, neurovascular connections. Roman numeral designations indicate cranial nerves. Scale bars equal 2 cm

the ophthalmic ($V_1$) and the maxillary ($V_2$) divisions of the trigeminal nerve pass through the sphenorbital fissure, whereas in *Bradypus* AMNH 95105 (Fig. 2j-l), the maxillary division extends through the foramen rotundum. This feature, observed in the encephalic cavity of *Glossotherium*, *Choloepus*, and *Bradypus*, agrees with the observations of Gaudin (2004) on the external surface of the skull in lateral view. In fact, the foramen rotundum is confluent with the sphenorbital fissure in most Mylodontidae (excluding *Nematherium* and *Pseudoprepotherium*) and also in *Choloepus*, *Eremotherium*, *Megatherium*, and *Thalassocnus*, whereas these two openings are separate in all the other sloths.

The foramen ovale, which accommodates the mandibular division ($V_3$) of the trigeminal, is present posterior and lateral to the sphenorbital fissure in all the examined specimens (Fig. 2).

More posteriorly, at the level of the petrosal bone, the internal acoustic meatus is pierced by the facial (VII) and vestibulocochlear (VIII) nerves (Fig. 2). The latter ends at the level of the inner ear, whereas the facial nerve has a more convoluted trajectory that has been reconstructed for *Glossotherium* (Fig. 3). Emerging from the primary facial foramen of the petrosal, the facial nerve forms the geniculate ganglion in the cavum supracochleare, just medial to the anteroventral process of the tegmen tympani, and anterior to the rostral end of the crista parotica. From this point, the facial nerve turns posteriorly, travels through the secondary facial foramen into the facial sulcus and, passing through the stylomastoid foramen, leaves the cranium ventrally (Fig. 3). Anterior to the geniculate ganglion, the greater petrosal nerve

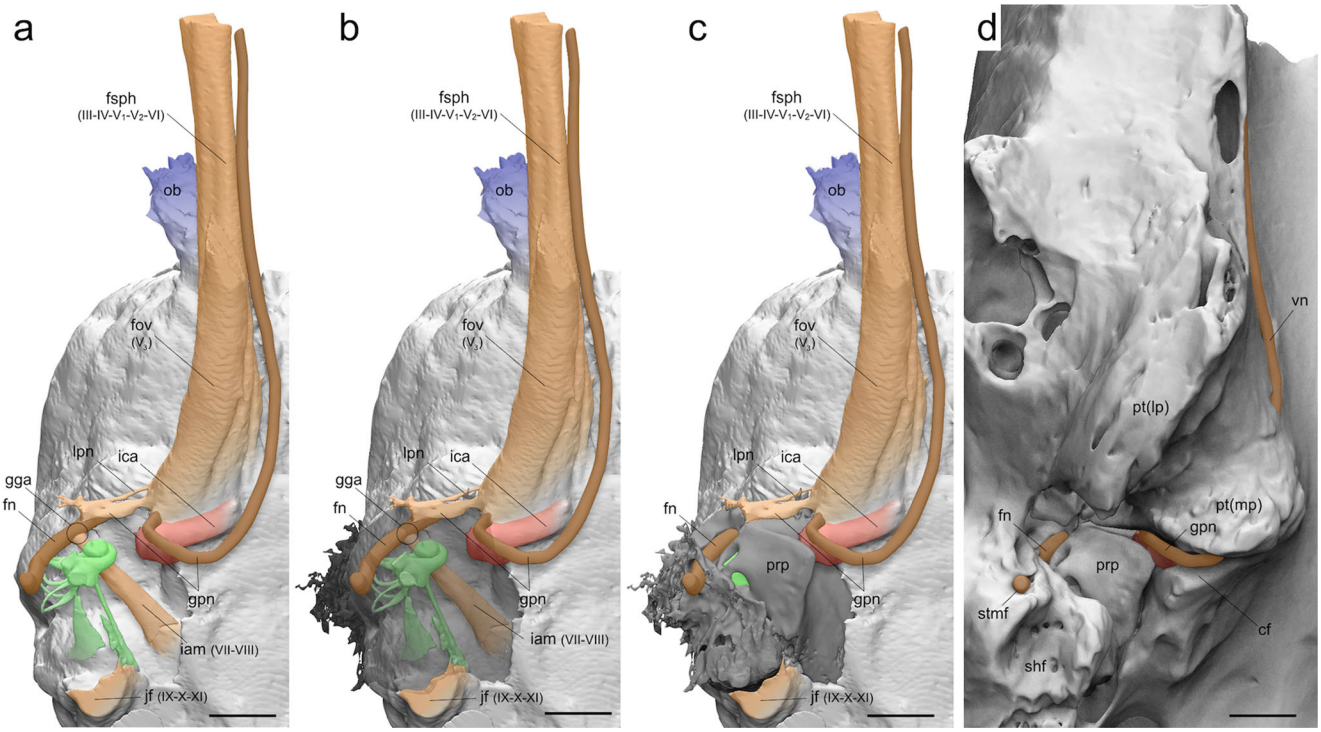


**Fig. 3** Digital reconstruction of (**a-c**) the right side endocasts in ventrolateral view, with the petrosal represented in decreasing degrees of opacity, and (**d**) the right side braincase in ventrolateral view, of *Glossotherium robustum* (MACN Pv 13553). Abbreviations: cf, carotid foramen; fn, facial nerve; fov, foramen ovale; fsph, sphenorbital fissure; gga, geniculate ganglion area; gpn, greater petrosal nerve; iam, internal acoustic meatus; ica, internal carotid artery; jf, jugular foramen; lpn, lesser petrosal nerve; ob, olfactory bulb; prp, promontorium of petrosal; pt(lp), pterygoid (lateral portion); pt(mp), pterygoid (medial portion); shf, stylohyal fossa; stmf, stylomastoid foramen; vn, vidian nerve. Colors indicate: blue, olfactory bulbs; green, bony labyrinth; orange, neurovascular connections; red, arterial vessels. Darker tones of red and orange indicate inferred structures on the outer surface of the skull. Roman numeral designations indicate cranial nerves. Scale bars equal 2 cm

turns medially and, after passing through the hiatus Fallopii, extends in a distinct sulcus on the epitympanic wing of the petrosal, before turning ventrally at the level of the trigeminal ganglion (Fig. 3). The greater petrosal nerve then enters in the foramen located in the anterior wall of the carotid foramen, piercing the ventral surface of the medial portion of the pterygoid and emerging anteriorly in the groove of the vidian nerve (Fig. 3). The lesser petrosal nerve is an anterior extension of the tympanic nerve (a branch of the glossopharyngeal nerve, cranial nerve IX, that forms a sensory tympanic plexus on the ventral surface of the promontorium; Clemente 1985; Evans 1993; Wible 2010). The tympanic nerve leaves no trace on the petrosal surface, but the lesser petrosal nerve enters a canal that extends parallel with but dorsal to the greater petrosal nerve (Fig. 3). The lesser petrosal nerve then follows the mandibular branch of the trigeminal nerve, and leaves the cranium through the foramen ovale.

More posteriorly, cranial nerves IX, X, and XI leave the braincase through the jugular foramen (Figs. 2 and 3).

The hypoglossal nerve (XII) is the most posterior cranial nerve, and is extremely well developed in *Glossotherium* (Fig. 2a-c), but very reduced in the extant sloths (Fig. 2e-l).

In general, *Glossotherium* exhibits great enlargement of the sphenorbital fissure, the foramen ovale, and the hypoglossal foramen, in comparison with all the other nerve-transmitting foramina (Fig. 2a-d). On the contrary, more homogeneity in the size of the foramina is observed in the extant sloths *Choloepus* (Fig. 2e-h) and *Bradypus* (Fig. 2i-l).

## Blood Vessels

As already observed, the surface of the brain endocast of *Glossotherium* is more rugose and convoluted than in the extant sloths. Not only are sulci and gyri more evident in *Glossotherium* than in the extant genera, but grooves for the blood vessels are also more clearly marked. In fact, some vessels have left marks that we attribute to both arteries and veins (Fig. 4).

**Arteries** The main arterial vessel leading to the brain is the internal carotid artery, entering in the cranial cavity though the carotid foramen, located at the anteromedial corner of the petrosal. In *Glossotherium*, the track of the internal carotid artery is particularly enlarged at the base of the trigeminal ganglion, and is visible on both sides of the ventral surface of the endocast, at the level of the hypophyseal reagion (Fig. 4b–d). This vessel is partially visible in the ventral endocast of *Choloepus* (Fig. 4f) but not detectable in *Bradypus*. In both *Glossotherium* and *Choloepus*, the internal carotid artery shows a strong posterolateral to anteromedial trajectory, following a detached sulcus on the internal side of the petrosal (Patterson et al. 1992; Boscaini et al. 2018). In *Glossotherium* (Fig. 4a, b, d), two paired arteries diverge toward the olfactory bulbs (= internal ethmoidal arteries, according to Evans 1993: 626). These are partially preserved in *Glossotherium* MACN Pv 13553 along the medial margin of the olfactory bulbs, and are oriented largely dorsoventrally (Fig. 4a, b, d).

These vessels are attributed to arteries on the basis of their large size, which is more compatible with the anteriormost termination of the ventral arterial system of the brain than any vein draining the region. Moreover, this pattern is typical in mammals and appears to be plesiomorphic in xenarthrans, as it is observed in the extant armadillos, anteaters, and sloths (Hyrtl 1854; Tandler 1901; Bugge 1979).

**Veins** The venous circulation is partially preserved in MACN Pv 13553. In dorsal view, some tiny vessels, the branches of the frontal meningeal veins, depart from the olfactory bulbs and are posteriorly directed (Fig. 4a, c, d). More posteriorly, the branches of the parietal meningeal vein are thicker than the frontal meningeal veins and are irregularly distributed. All these veins are confluent with the dorsal sagittal sinus, the posteriormost portion of which is represented in MACN Pv 13553 (Fig. 4a). This latter sinus is observable along nearly its entire length in *Oreomylodon* (Dechaseaux 1971). The dorsal sagittal sinus connects posteriorly to the paired transverse sinuses at the level of their median divergence (Fig. 4; Evans 1993: 709). The grooves for these latter vessels, located at the boundary between the cerebral hemispheres and the cerebellum (and thus along the transverse fissure), are the deepest on the dorsal surface of the endocast, a condition that is also observed in other extinct sloths such as *Megatherium*, *Mylodon*, *Oreomylodon*, *Scelidotherium*, and *Eucholoeops* (Gervais 1869; Dechaseaux 1958, 1962a, 1971; Dozo 1994).

In lateral view, the transverse sinus gives rise laterally into two anteriorly directed lesser veins: the ventral cerebral vein and the dorsal petrosal sinus (Fig. 4c). The former has a wider diameter than the latter, and extends partially in the caudal suprasylvian sulcus, whereas the latter is narrower, lies in a more ventral position (on the pyriform lobe), and projects farther anteriorly (Fig. 4c).

The greater part of the transverse sinus flows laterally and ventrally into the sigmoid sinus, which leaves the cranium through the jugular foramen (Fig. 4b, c). The sigmoid sinus is the only vein that is recognizable on the endocasts of the extant sloths *Choloepus* (Fig. 4e, h) and *Bradypus* (Fig. 4g, i). In its most ventral portion, the sigmoid sinus of *Glossotherium* MACN Pv 13553 is joined by two veins, the inferior petrosal sinus and the basilar sinus (Fig. 4b, c). In ventral view (Fig. 4b), the inferior petrosal sinus extends anteroposteriorly through a fissure that lies between the petrosal and the basioccipital. In its anteriormost portion the inferior petrosal sinus passes through a second opening in the posterior wall of the carotid foramen, whereas posteriorly it emerges in the anterior wall of the jugular foramen, where it joins the sigmoid sinus (Fig. 4b, c). There is a large branch of the inferior petrosal sinus that extends

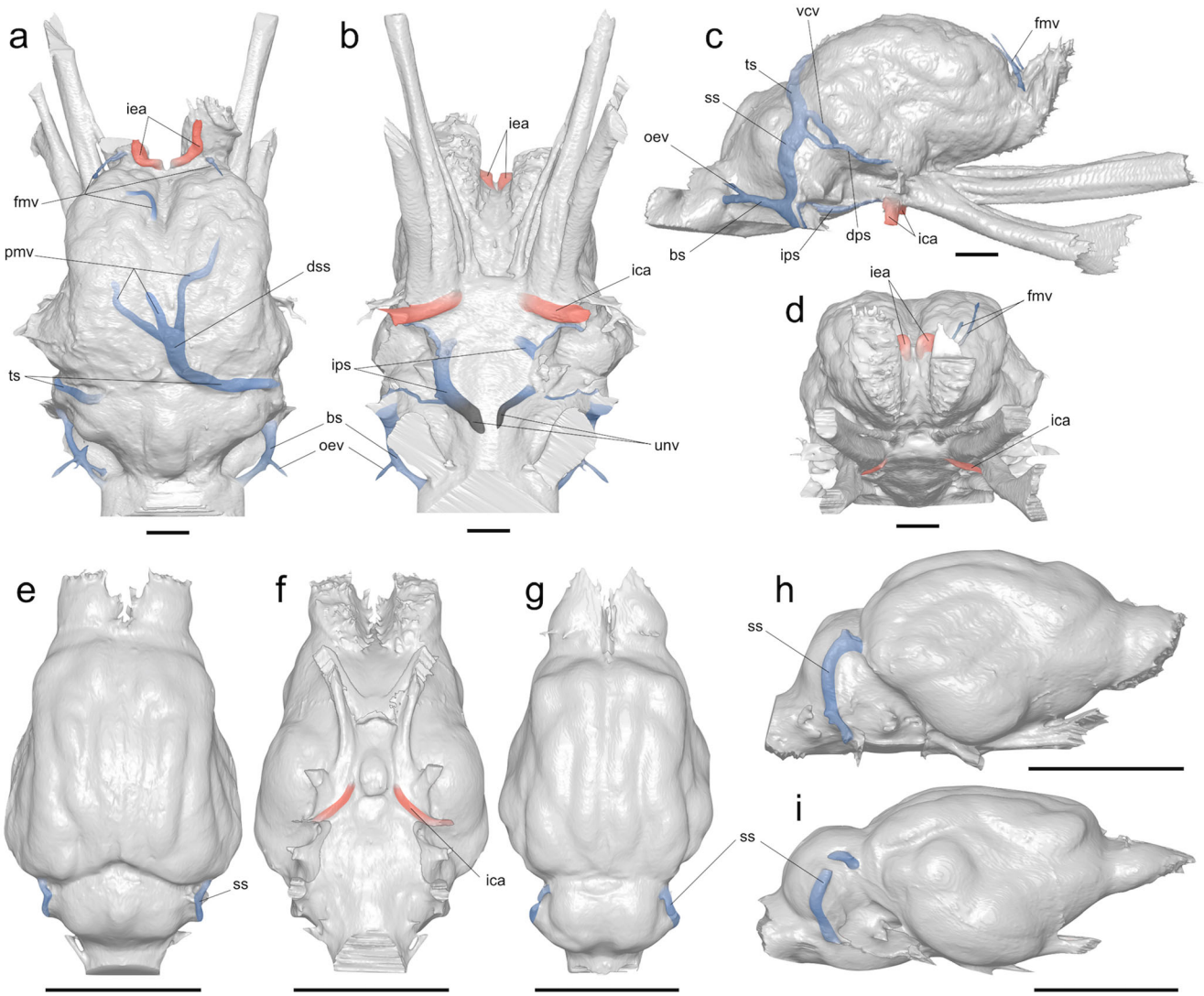


**Fig. 4** Brain endocasts of *Glossotherium* (MACN Pv 13553) (**a-d**), *Choloepus* (AMNH 30765) (**e, f, h**), and *Bradypus* (AMNH 95105) (**g, i**), in dorsal (**a**, **e**, **g**), ventral (**b**, **f**), lateral (**c**, **h**, **i**), and anterior (**d**) views, showing the arterial vessels (red) and venous vessels (blue). Abbreviations: bs, basilar sinus; dps, dorsal petrosal sinus; dss, dorsal sagittal sinus; fmv, branches of the frontal meningeal vein; ica, internal carotid artery; iea, internal ethmoidal artery; ips, inferior petrosal sinus; oev, occipital emissary vein; pmv, branches of the parietal meningeal vein; ss, sigmoid sinus; ts, transverse sinus; unv, unknown vessel; vcv, ventral cerebral vein. Scale bars equal 2 cm

posteroventromedially, the left and right sides converging toward the floor of the foramen magnum. We are unaware of a large vein that would occupy such a position in xenarthrans, or indeed in other mammals, so we have, for the time being, simply labeled this branch as an unknown vessel (Fig. 4b). The basilar sinus merges with the sigmoid sinus more dorsally than the inferior petrosal sinus, and extends through the condyloid canal (Fig. 4a-c). At its posterior end, the basilar sinus turns into the internal vertebral venous plexus as it leaves the foramen magnum (Evans 1993: 711). This condition was previously observed in the genus *Mylodon* by Patterson et al. (1992), who suggested that the "very large groove running from the inside of the foramen lacerum posterium to the foramen magnum" was pierced by an unidentified "venous sinus" (Patterson et al. 1992: 6). In accordance with the CT scans performed in the present study and the available literature (Clemente 1985; Evans 1993), this vein is likely the basilar sinus. The groove that housed this vessel is absent in all living xenarthrans (Patterson et al. 1992).

The condyloid canal, which connects the jugular foramen with the foramen magnum, has a dorsoposteriorly directed branch near its caudal end (Fig. 4a-c). This branch emerges posteriorly at the mastoid foramen, located just dorsal to the occipital condyle. This latter canal accommodated the occipital emissary vein, draining the external surface of the occipital bone.

## Paranasal Pneumaticity

The paranasal sinuses, a characteristic feature of placental mammals (e.g., Moore 1981; Novacek 1993), are air-filled chambers

that form within a variety of cranial bones and are connected to the nasal cavity. They are commonly divided into maxillary, frontal, and sphenoidal sinuses, of which the maxillary sinuses are the most basal and widespread among eutherian mammals (Moore 1981). The maxillary sinuses are also invariably present in xenarthrans (Moore 1981). Unfortunately, due to breakage of the anterior portion of MACN Pv 13553 (Fig. 1), the maxillary sinuses cannot be observed. Thus, the description and comparison that follow will be limited to the frontal and sphenoidal sinuses. These sinuses are so named because they are typically found within the frontal and sphenoidal bones (specifically the presphenoid; Evans 1993), but sometimes they extend into other cranial bones (Moore 1981). For this reason, and following this scheme, our description of the cranial pneumatization pattern in *Glossotherium* and the extant sloth genera will be based on the bony elements directly involved (thus, for example, we refer to the orbitosphenoid sinus). In mammals, the number and extent of the chambers differ among species, but their development also varies greatly during ontogeny, producing intraspecific variation among individuals of different ages, particularly during the later stages of growth and in adult life (Moore 1981; Farke 2008). Moreover, minor differences occur between the right and left sides of a single individual (Moore 1981). Therefore, our descriptions are limited to symmetrically observed aspects of sinus morphology, and our inter-taxon comparison is made only among adult specimens, in order to avoid differences related to different ontogenetic stages.

The three genera considered in this work (i.e., *Glossotherium*, *Choloepus*, and *Bradypus*) possess both frontal and orbitosphenoid sinuses. In *Bradypus*, the frontal sinuses are smooth walled and shallow in lateral view (Fig. 5g-i). These sinuses are approximately rectangular in

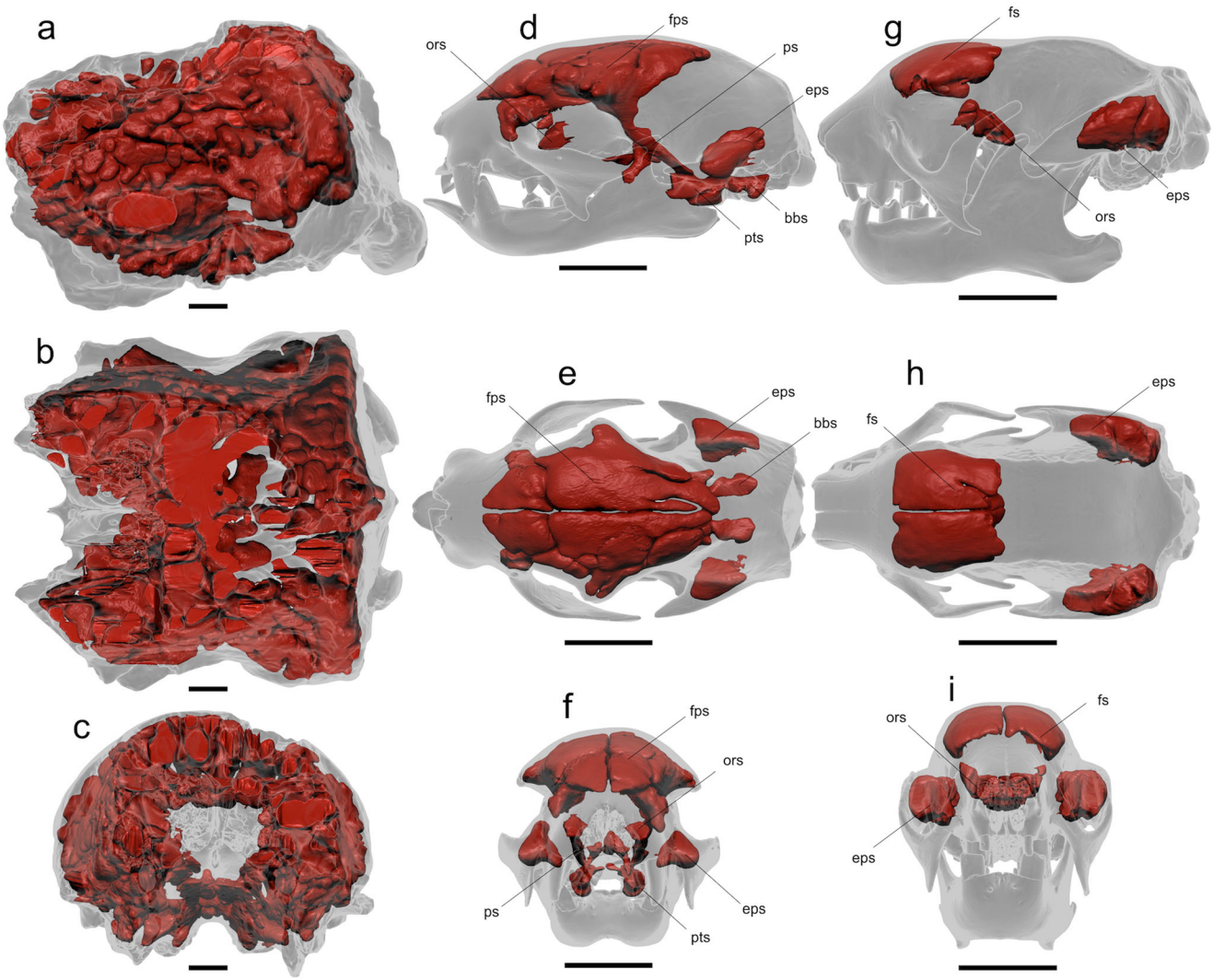


**Fig. 5** Paranasal pneumaticity in the skulls of *Glossotherium* (MACN Pv 13553) (**a-c**), *Choloepus* (AMNH 30765) (**d-f**), and *Bradypus* (AMNH 95105) (**g-i**), in lateral (**a**, **d**, **g**), dorsal (**b**, **e**, **h**), and anterior (**c**, **f**, **i**) views. Abbreviations: bbs, basisphenoid-basioccipital sinuses; eps, epitympanic sinuses; fps, fronto-parietal sinuses; fs, frontal sinuses; ors, orbitosphenoid sinuses; ps, palatine sinuses; pts, pterygoid sinuses. Scale bars equal 2 cm

dorsal view and more elongated anteroposteriorly than mediolaterally. They are composed of a single chamber that covers the olfactory bulbs dorsally and is limited posteriorly by the fronto-parietal suture (Fig. 5g, h). Ventral to, and separate from the frontal sinuses, some small sinuses open into the orbitosphenoid. These orbitosphenoid sinuses are located just ventral to the olfactory bulbs and posterior to the ethmoid. Their most lateral portions project anteriorly towards the nasopharynx (Fig. 5g). Another highly pneumatized part of the skull is the zygomatic process of the squamosal, which contains the epitympanic sinus, passing dorsally from its posterior connection to the tympanic cavity into the squamosal, and then extending anteriorly to the level of the glenoid fossa (Fig. 5g, h). Also, large pterygoid sinuses have been described in the maned sloth, *B. torquatus* (e.g., Guth 1961), but are not evident in our specimen of *B. variegatus*, and are not known to be developed in other *Bradypus* species (Patterson et al. 1992; Hayssen 2008, 2010). The frontal, orbitosphenoid, and zygomatic sinuses are distinct and well separated in lateral, dorsal, and anterior views (Fig. 5g–i).

In *Choloepus* (Fig. 5d-f), the frontal sinuses are much larger, more complex, more convoluted, and display more bilateral asymmetry than those of *Bradypus* (Fig. 5g–i). In the two-toed sloth, these sinuses are composed of several chambers extending dorsally over the olfactory bulbs (Fig. 5d-f). In dorsal view (Fig. 5e), they extend posterior to the fronto-parietal suture into the parietal, following an irregular pattern that is not observed in *Bradypus* (Fig. 5h).

*Choloepus* has small orbitosphenoid sinuses that are visible in lateral and anterior views, just ventral to the olfactory bulbs (Fig. 5d, f). These are separated from the frontal sinuses, as in *Bradypus*. In their most lateral parts they project anteriorly, but are quite asymmetric (Fig. 5d, f). In contrast with *Bradypus*, the frontal sinuses of *Choloepus* project markedly posteroventrally in lateral and anterior views. This extension merges with the palatine sinuses (Fig. 5d, f). On the right side of *Choloepus* AMNH 30765, the pneumatization is continuous, whereas it is separated by a thin septum on the left side (Fig. 5d, f). More ventrally, the pneumatization of the palatine is in contact with the pterygoid sinuses in both the right and the left sides. The inflation of the pterygoid is more pronounced in *Choloepus* than in *Bradypus* (except in *B. torquatus*, see preceding paragraph) or *Glossotherium* (Gaudin 2004: char 137). The basicranial pneumatization extends posteriorly into the basisphenoid and the basioccipital, again with a sinuous and irregular pattern comparable to the irregularities observed in the other sinuses of *Choloepus*. As in *Bradypus*, the zygomatic process of the squamosal is also well pneumatized, housing an extensive epitympanic sinus (Fig. 5d-f). The pneumatized region extends from the tympanic cavity dorsally into the squamosal and anteriorly to the level of the glenoid fossa, but it tapers in width posteriorly, terminating before reaching the posterior end of the zygomatic process. Therefore, the epitympanic sinus is somewhat smaller and more anteriorly restricted than that of *Bradypus* (Fig. 5d-e, g-h). *Choloepus* displays more pneumatized areas than *Bradypus*, as well as more communication among them (Fig. 5d-f, g-i).

In *Glossotherium* (MACN Pv 13553; Fig. 5a-c) the pneumatization is so pervasive that the sinuses mirror the external morphology of the cranium and are not separable into well-defined areas as in *Choloepus* (Fig. 5d-f) and *Bradypus* (Fig. 5g-i). Pneumatization in *Glossotherium* affects the whole braincase, from the occipital to the parietals and frontals, extending ventrally into the side walls of the braincase and the basicranium, and supported throughout by internal struts (Figs. 1a, 5a-c). This condition is comparable to the extent of pneumatization in other extinct giant sloths in which this feature has been observed, such as the mylodontid *Oreomylodon* and the megalonychids *Megalocnus* and *Megistonyx* (Dechaseaux 1971; Patterson et al. 1992; McDonald et al. 2013). However, such pneumatization may not be universal in giant extinct sloths, as suggested by the genus *Eremotherium* (see sectioned skull in Patterson et al. 1992: 35). In lateral view, air-filled chambers are missing from only a few areas of the skull of *Glossotherium*. These include the paraoccipital process of the petrosal and the exoccipital crest, both involved in the formation of the stylohyal fossa (Fig. 5a, b). Also, the bones surrounding the foramen magnum are not pneumatized, including the most distal portion of the basioccipital and the most ventral limit of the occipital, along with the occipital condyles (Fig. 5a, b). This is probably related to the robustness necessary in these areas that articulate with the hyoid apparatus and the vertebral column, respectively. A reduction of the sinuses in the vicinity of the foramen magnum is also observed in modern elephants, the cranium of which is otherwise highly pneumatized (Van der Merwe et al. 1995). Left and right portions of the cranium in *Glossotherium* display similar pneumatization, but there is considerable shape variation. Some tubular structures are detectable among the rounded air-filled spaces, both on the internal and external sides of the pneumatized layer. These structures are neurovascular in nature, but their limits frequently cannot be traced because of breakage or structural discontinuities.

## Discussion

The recent increase in paleoneurological studies of extant and fossil vertebrates reflects the fact that brain endocasts represent an important source of anatomical, morpho-functional, and, in particular cases, ethological information, which help researchers in their attempt to better understand the paleobiology of fossil mammals (e.g., Sakai et al. 2011; Cunningham et al. 2014; Thiery and Ducrocq 2015; Dozo and Martínez 2016; Vinuesa et al. 2016; Bertrand et al. 2017). Unfortunately, our knowledge of fossil sloth brain morphology and its functional

implications are based on only a very few, dated studies (e.g., Gervais 1869; Dechaseaux 1971; Dozo 1987, 1994). In addition, endocasts from this group of fossil mammals have been obtained from only a limited number of genera, almost always represented by very few specimens. Despite these limitations, the descriptions and comparisons of the endocast features in the present study allow for some preliminary analysis.

**Brain Endocast** According to Dechaseaux (1971) and Dozo (1987), all the fossil sloth taxa discussed above show a very similar brain morphology, and this similarity involves not only the general shape of the brain, but also the pattern of convolutions, which are highly conservative in both extinct and extant sloth species. However, the apparent roughness of the external surface is shared exclusively among the large-bodied extinct sloths, suggesting that this feature might be related to allometric factors. The pattern of convolutions apparently remained fairly stable during the evolutionary history of sloths and the number, and arrangement, of the identified convolutions is almost the same (Fig. 2). In both *Glossotherium* MACN Pv 13553 and A10.263, the entolateral sulcus is clearly visible, but this is also true in the extinct genera *Lestodon*, *Megatherium, Mylodon, Oreomylodon*, and *Scelidotherium* (Gervais 1869; Dechaseaux 1958, 1962a, 1971), and in the extant two-toed sloth *Choloepus*. However, this sulcus is absent in the extant three-toed sloth *Bradypus* and in the middle Miocene forms *Hapalops* and *Eucholoeops* (Dozo 1987, 1994). The distribution of this feature accords with the most recent phylogenetic scenarios based on morphological evidence (Gaudin 1995, 2004), which propose that *Choloepus* and *Glossotherium* are more closely related to one another than either is to *Bradypus*. However, the condition in *Bradypus* is present in *Hapalops* and *Eucholoeops*, even though the latter two are more closely related to *Choloepus* than *Glossotherium* according to Gaudin (2004). The simplified pattern of *Bradypus*, *Hapalops*, and *Eucholoeops*, along with the phylogenetic position of *Bradypus* as the putative sister-taxon to all other sloths, suggests that *Bradypus* has maintained the plesiomorphic condition probably since the Oligocene (Dozo 1987, 1994; Gaudin and Croft 2015), but it may also imply that the similarity between *Glossotherium* and *Choloepus* evolved convergently.

The complexity of convolutions is generally higher in large-sized mammals than in medium- to small-sized mammals, because the convolutions increase the amount of cortical surface area, compensating for reductions in surface area to volume ratio for brains of increasing size (e.g., Prothero and Sundsten 1984; Roth and Dicke 2005; Macrini et al. 2007b). Folivorans seemingly do not follow this rule. In fact, the apparent complexity of the telencephalic surface in *Glossotherium* and other large-sized species is related to the presence of several surface irregularities, consisting of a high number of recesses and protrusions (Fig. 2). Their irregular shape, small size, and, especially, uniform distribution on the brain surface (they are even observed on surfaces of the blood vessels) allow us to exclude the possibility that these structures are convolutions. They are more likely interpreted as traces of meninges. In large extant mammals of similar size (e.g., pachyderms and cetaceans), meninges, cisterns, and other soft-tissue structures tend to fill the spaces in the sulci of the brain, obscuring the pattern of sulci and gyri (Macrini et al. 2007b and references therein) and this phenomenon can be partially responsible for the reduced sulcation in *Glossotherium*. In any case, in extant and extinct sloths the basic pattern of convolutions is always observable, independent of body size. This basic pattern closely resembles that of carnivorans, which display the simplest arrangement of convolutions among gyrencephalic mammals (Barone and Bortolami 2004). This similarity is particularly strong for the dorsal surface of the telencephalon, and has been previously reported by Gervais (1869), Elliot-Smith (1898), and Anthony (1953).

The olfactory bulbs in *Glossotherium* strongly project dorsally (Fig. 2a-d), with an enlarged anterior surface covered by the many ramifications of the olfactory nerve. In the specimens of *Oreomylodon* and *Glossotherium* figured by Dechaseaux (1958, 1971), the olfactory bulbs are also directed and enlarged dorsally. Even though the splanchnocranial portion is missing in *Glossotherium* MACN Pv 13553, a fragment of the ethmoid bone is preserved, and in it the cribriform plate appears vertical, exceeding in height the dorsal portion of the olfactory peduncles. This condition is also observed in *Oreomylodon* (Dechaseaux 1971: fig. 5), but it does not occur in the extant sloth taxa, where the cribriform plate ends at the dorsal limit of the olfactory peduncles, thus conferring a horizontal dorsal profile to the bulbs in lateral view. In *Glossotherium*, the dorsal projection of the olfactory bulbs can be related to the dorsoventral expansion of the nasal cavities, which can affect the horizontal development of the cribriform plate and, consequently, the vertical profile of the bulbs. It is currently difficult to assess if, and how, this peculiar morphology of the olfactory bulbs relates to the olfactory sensitivity in this extinct sloth. For example, the expansion of the nasal cavities may represent an adaptation to particular environmental conditions, or may be related to thermoregulation, water balance, or even sound production (or a combination of them). A larger set of cranial and paleoneurological data is needed to better understand the correlation between morphology and function of the olfactory bulbs in these taxa. A dorsal projection of the olfactory bulbs is not present in *Choloepus*, but like *Glossotherium*, it has anteroposteriorly short bulbs that are deep dorsoventrally and narrow transversely. The olfactory bulbs of *Bradypus* are shallow dorsoventrally, elongated anteroposteriorly, and pointed at their anterior tip, with a broad olfactory peduncule, imparting a morphology quite different from that observed in *Glossotherium* and *Choloepus*. The shape of the olfactory bulbs in *Bradypus* does resemble that of *Hapalops* (Dozo 1987), and to a lesser

extent of *Eucholoeops* (Dozo, 1994), which again likely represents the retention of a plesiomorphic condition in these taxa.

If the telencephalon shows a fairly uniform pattern of convolutions in both extinct and extant sloths, the cerebellum (together with the olfactory bulbs) represents the most variable portion of the sloth endocasts. In dorsal view, *Glossotherium* has a subtriangular cerebellum with the apex formed by the posterior portion of the vermis. This shape is the result of a lateral expansion of the two cerebellar hemispheres, which reach a maximum transverse width equivalent to that of the posterior portions of the cerebral hemispheres. This latter is a common feature in large-bodied extinct sloths, and is generally accompanied by the presence of a well-developed paraflocculus. The presence of large paraflocculi is considered a plesiomorphic character within therian mammals (Kielan-Jaworowska 1986; Macrini et al. 2007b). In *Glossotherium*, the parafloccular areas are proportionally wider than in the small-bodied extant sloths *Bradypus* and *Choloepus*, in which they appear as tiny swellings just dorsal to the jugular foramen (Fig. 2). The former condition was previously illustrated by Dechaseaux (1971) for both *Glossotherium* and *Oreomylodon*. The latter condition is here reported for the two extant genera *Choloepus* and *Bradypus,* but was also recognized in the late early Miocene sloths *Hapalops* and *Eucholeops* (Dozo 1987, 1994). Further studies should investigate the possible allometric and functional significance of this feature.

**Cranial Nerves** The main trajectories of the cranial nerves have been reconstructed for *Glossotherium robustum* MACN Pv 13553 (Figs. 2 and 3) and the extant sloths *Bradypus* and *Choloepus* (Fig. 2). The cranial nerve pathways through the sphenorbital fissure, foramen rotundum, and foramen ovale are similar in *Glossotherium* and *Choloepus*, and differ significantly from the pattern in *Bradypus*, consistent with their proposed closer phylogenetic affinity (Gaudin 1995, 2004). In *Glossotherium*, we observed that the grooves for the sphenorbital fissure, the foramen ovale, and the hypoglossal foramen are enlarged relative to other foramina transmitting cranial nerves, confirming initial observations by Owen (1839, 1842). The presence of these deep furrows is probably related to a greater development of the trigeminal and hypoglossal nerves, compared to other nerves, in the extinct sloth *Glossotherium*, than in *Bradypus* and *Choloepus*, where the nerve-transmitting foramina are more uniform in size. This probably can be related to larger relative sizes of tongue and jaw muscles in the extinct genus *Glossotherium* than the extant forms, in accordance with their different dietary habits (Bargo et al. 2006b; Pujos et al. 2012). The large sphenorbital fissure and foramen ovale also could be partially related to an increased sensory innervation coming from the elongated rostrum and enlarged nasal cavity of *Glossotherium*.

**Blood Vessels** Blood vessels are more difficult to observe in the small-sized extant sloths than the large-sized *Glossotherium* (Fig. 4). In the latter (Fig. 4a-d) many blood vessels are discernible, and the general pattern is similar to that observed in other extinct sloths (Gervais 1869; Dechaseaux 1958, 1962a, 1971; Dozo 1994) and comparable with the plesiomorphic condition in xenarthrans (Hyrtl 1854; Tandler 1901; Bugge 1979). This suggests a conservative conformation of the blood circulation. The sigmoid sinus is the only vessel that is invariably observed in *Glossotherium*, *Choloepus*, and *Bradypus*, whereas the impression of the internal carotid artery is another feature only found in *Glossotherium* and *Choloepus* (Fig. 4).

**Paranasal Pneumatization** Many hypotheses concerning the function of the paranasal sinuses have been proposed (exhaustive reviews are available in Blanton and Biggs 1969; Moore 1981; Blaney 1990). The idea that cranial pneumatization is basically functionless (Weidenreich 1924, 1941; Edinger 1950; Witmer 1997) has become the most widely accepted hypothesis over the last decade (Farke 2008, 2010). The possible existence of "opportunistic pneumatization," which implies that the sinuses do not have any apparent function and are merely the result of the removal of structurally unnecessary bone, has been gaining support over the last few years and was recently advocated by Farke (2007, 2008, 2010) who conducted the "broadest and most comprehensive quantitative analysis of sinus morphology ever attempted" (Farke 2010: 1010). The same author demonstrated that the size and complexity of paranasal sinuses in bovids are not related with their ramming behavior, as previously thought (Farke 2010). On the contrary, they seem to be partially related to the size of the frontals (and consequently the whole skull), and consistent with a role for the sinuses in weight reduction (Farke 2010). However, this is true only in those groups that already possess pneumatized frontal bones, suggesting both a positive allometry with skull size and a strong phylogenetic component. In this sense, Farke (2010) recognized that the presence of a frontal sinus is the ancestral condition in Bovidae and has been lost several times during the evolution of the clade. In different bovid taxa, Farke (2010) also detected several pneumaticity patterns, which include: i) sinuses extending up to the fronto-parietal suture (i.e., sinuses that do not cross the suture and even conform to its morphology), ii) sinuses extending beyond the fronto-parietal suture to pneumatize the parietal, and occasionally also the occipital bone, and iii) sinuses widely extended and pneumatizing large regions of the cranium (e.g., including the entirety of the horn cores).

Our preliminary data suggest that similarities between bovids and sloths can be recognized regarding the development of the sinuses. Generally, sinus morphology in Xenarthra seems to have a strong phylogenetic component, given that frontal sinuses have been demonstrated to be diagnostic even at the subspecific level for different morphotypes of the nine-banded armadillo *Dasypus novemcinctus* (Billet et al. 2017). In contrast, frontal sinuses are lacking in anteaters, in which

only some basicranial pneumatizations are observed, mainly in the alisphenoid, palatine, and the pterygoid bones, along with an epitympanic sinus in the squamosal (Moore 1981; Storch and Habersetzer 1991; Patterson et al. 1992; Gaudin 1995, 2004).

In the three sloth genera described in the present study, the frontal sinuses are invariably present. *Bradypus*, the putative sister group to all the other extant and extinct sloths (e.g., Gaudin 2004) presents the simplest observed pattern, with the fronto-parietal suture limiting the extent of the frontal sinuses posteriorly (Fig. 5g–i). On the other hand, *Glossotherium* and *Choloepus*, which are more closely related phylogenetically according to Gaudin (2004), also show similarities exclusive of *Bradypus* in the morphology of their cranial sinuses. For example, both exhibit a continuous pneumatization, from the frontals to the basicranium (Fig. 5a–f). This pneumatization is extremely exaggerated in *Glossotherium,* so that it involves a series of interconnected chambers invading nearly every posterior cranial bone. Total body size must be taken into account, and we note that *Bradypus* is the smallest of the three genera, followed closely by *Choloepus*, whereas *Glossotherium* is much larger, approaching the size of the largest modern bovids. This suggests the presence of a corresponding positive allometry in sinus size relative to skull size. As Farke (2010) observed in bovids, it appears that in the sloth clade, the different patterns observed are likely related to both phylogenetic effects and the influence of body size.

## Conclusions

The digital cranial endocasts of *G. robustum* have been described and compared with representative specimens of extant sloths, providing an anatomical characterization of the main features of the brain cavity, cranial nerves, blood vessels, and paranasal sinuses.

Among these structures, we detected features that could have a phylogenetic signal, such as the general shape of the brain endocast, the presence/absence of the entolateral sulcus, and the shape of the olfactory bulbs and the vermis. However, the general pattern of sulci and gyri on the brain endocast appeared to be extremely conservative in the folivoran clade and we confirmed its simple organization, independent of body size, if compared with other mammals. Similarly, the arterial and venous circulation appeared to be conservative in sloths, even if blood vessel features are more difficult to observe in smaller- rather than larger-sized sloths. Other characters, such as the apparent roughness of the external surface of the brain endocast and the mediolaterally expanded cerebellum, may be related, instead, to allometric factors. In contrast, the relative size of the foramina through which the trigeminal and hypoglossal nerves passed suggests a probable physiological influence, related with food processing and sensory information.

Finally, paranasal pneumatization shows evidence of mixed signals, i.e., it is mainly affected by phylogenetic and allometric factors, even if a functional influence related to body size increase cannot be currently refuted.

The anatomical regions of the extinct sloth *G. robustum* analyzed in this work under 3D imaging techniques show the great potential of these methodologies for elucidating the evolutionary history of this peculiar mammalian clade.

**Acknowledgments** We are grateful to the FUESMEN for access to CT-scanning facilities, and in particular we are indebted to Sergio Mosconi and collaborators for assistance with image processing. We thank A. Kramarz, S.M. Alvarez, and L. Chornogubsky (MACN) who kindly gave access to the specimens under their care. This work was possible thanks to the facilities offered by the PaleoFactory Lab (Sapienza Università di Roma, Rome, Italy) and the free digital database available at http://digimorph.org. We also want to thank G. Billet, L. Hautier, M. Fernández-Monescillo, S. Hernández del Pino, and A. Forasiepi for their useful suggestions. This paper greatly benefited from the careful reading and thoughtful comments by the Editor J.R. Wible and two anonymous reviewers. This work was partially funded by ECOS-FonCyT (A14U01).

## References

Ameghino F (1889) Contribución al conocimiento de los mamíferos fósiles de la República Argentina. Actas Acad Nac Ciencias Córdoba 6:1–1027

Anthony J (1953) Morphologie externe du télencéphale dans le genre *Bradypus* L. (Edentata). Mammalia 17(3):1–149

Antoine PO, Marivaux L, Croft DA, Billet G, Ganerød M, Jaramillo C, Martin T, Orliac MJ, Tejada J, Altamirano AJ, Duranthon F, Fanjat G, Rousse S, Salas Gismondi R (2012) Middle Eocene rodents from Peruvian Amazonia reveal the pattern and timing of caviomorph origins and biogeography. Proc R Soc B-Biol Sci 279:1319–1326

Antoine PO, Salas-Gismondi R, Pujos F, Ganerød M, Marivaux L (2017) Western Amazonia as a hotspot of mammalian biodiversity throughout the Cenozoic. J Mammal Evol 24(1): 5–17

Bargo MS, De Iuliis G, Vizcaíno SF (2006a) Hypsodonty in Pleistocene ground sloths. Acta Palaeontol Pol 51(1):53–61

Bargo MS, Toledo N, Vizcaíno SF (2006b) Muzzle of South American Pleistocene ground sloths (Xenarthra, Tardigrada). J Morphol 267: 248–263

Bargo MS, Vizcaíno SF (2008) Paleobiology of Pleistocene ground sloths (Xenarthra, Tardigrada): biomechanics, morphogeometry and ecomorphology applied to the masticatory apparatus. Ameghiniana 45(1):175–196

Bargo MS, Vizcaíno SF, Archuby FM, Blanco RE (2000) Limb bone proportions, strength and digging in some Lujanian (Late Pleistocene-Early Holocene) mylodontid ground sloths (Mammalia: Xenarthra). J Vertebr Paleontol 20(3):601–610

Barone R, Bortolami R (2004) Anatomie comparée des mammifères domestiques. Tome 6, Neurologie I, Système Nerveux Central. Vigot Frères, Paris

Bergqvist LP, Abrantes EAL, Avilla LDS (2004) The Xenarthra (Mammalia) of São José de Itaboraí Basin (upper Paleocene, Itaboraian), Rio de Janeiro, Brazil. Geodiversitas 26(2):323–337

Bertrand OC, Amador-Mughal F, Silcox MT (2017) Virtual endocast of the early Oligocene *Cedromus wilsoni* (Cedromurinae) and brain evolution in squirrels. J Anat 230(1):128–151

Billet G, Hautier L, de Thoisy B, Delsuc F (2017) The hidden anatomy of paranasal sinuses reveals biogeographically distinct morphotypes in the nine-banded armadillos (*Dasypus novemcinctus*). PeerJ Preprints 5:e2923v1 https://doi.org/10.7287/peerj.preprints.2923v1

Blanco RE, Rinderknecht A (2008) Estimation of hearing capabilities of Pleistocene ground sloths (Mammalia, Xenarthra) from middle-ear anatomy. J Vertebr Paleontol 28(1):274–276

Blanco RE, Rinderknecht A (2012) Fossil evidence of frequency range of hearing independent of body size in South American Pleistocene ground sloths (Mammalia, Xenarthra). C R Palevol 11(8):549–554

Blaney SPA (1990) Why paranasal sinuses? J Laryngol Otol 104:690–693

Blanton PL, Biggs NL (1969) Eighteen hundred years of controversy: the paranasal sinuses. Am J Anat 124:135–148

Bocquentin J (1979) Mammifères fossiles du Pléistocène supérieur de Muaco, État de Falcón, Venezuela. Dissertation, Université Pierre et Marie Curie

Boscaini A, Iurino DA, Billet G, Hautier L, Sardella R, Tirao G, Gaudin TJ, Pujos F (2018) Phylogenetic and functional implications of the ear region anatomy of *Glossotherium robustum* (Xenarthra, Mylodontidae) from the late Pleistocene of Argentina. Sci Nat https://doi.org/10.1007/s00114-018-1548-y

Bugge J (1979) Cephalic arterial pattern in New World edentates and Old World pangolins with special reference to their phylogenetic relationships and taxonomy. Acta Anat 105:37–46

Christiansen P, Fariña RA (2003) Mass estimation of two fossil ground sloths (Mammalia, Xenarthra, Mylodontidae). Senckenb Biol 83(1): 95–101

Clemente CD (1985) Gray's Anatomy. Lea and Febiger, Philadelphia

Constantinescu GM, Schaller O (2012) Illustrated Veterinary Anatomical Nomenclature. Enke Verlag, Stuttgart

Cope ED (1889) The Edentata of North America. Am Nat 23(272):657–664

Cunningham JA, Rahman IA, Lautenschlager S, Rayfield EJ, Donoghue PC (2014) A virtual world of paleontology. Trends Ecol Evol 29(6): 347–357

Czerwonogora A, Fariña RA, Tonni EP (2011) Diet and isotopes of late Pleistocene ground sloths: first results for *Lestodon* and *Glossotherium* (Xenarthra, Tardigrada). Neues Jahrb Geol Palaontol Abh 262(3):257–266

Dechaseaux C (1958) Encéphales de xénarthres fossiles. In: Piveteau J (ed) Traité de Paléontologie. Masson and Cie, Paris, pp 637–640

Dechaseaux C (1962a) Encéfalos de Notongulados y de Desdentados Xenarthros Fósiles. Ameghiniana 2(11):193–209

Dechaseaux C (1962b) Singularités de l'encéphale de *Lestodon*, mammifère édenté géant du Plésitocène d'Amérique du Sud. C R Acad Sci 254:1470–1471

Dechaseaux C (1971) *Oreomylodon wegneri*, édenté gravigrade du Pléistocène de l'Équateur - Crâne et moulage endocrânien. Ann Paleontol 57(2):243–285

De Iuliis G, Cartelle C, McDonald HG, Pujos F (2017) The mylodontine ground sloth *Glossotherium tropicorum* from the late Pleistocene of Ecuador and Peru. Pap Palaeontol: https://doi.org/10.1002/spp2.1088

Delsuc F, Catzeflis FM, Stanhope MJ, Douzery EJ (2001) The evolution of armadillos, anteaters and sloths depicted by nuclear and mitochondrial phylogenies: implications for the status of the enigmatic fossil *Eurotamandua*. Proc R Soc B 268(1476):1605–1615

Dozo MT (1987) The endocranial cast of an early Miocene edentate, *Hapalops indifferens* Ameghino (Mammalia, Edentata, Tardigrada, Megatheriidae). Comparative study with brains of recent sloths. J Hirnforsch 28(4):397–406

Dozo MT (1994) Interpretación del molde endocraneano de *Eucholoeops fronto*, un Megalonychidae (Mammalia, Xenarthra, Tardigrada) del Mioceno temprano de Patagonia (Argentina). Ameghiniana 31(4): 317–329

Dozo MT, Martínez G (2016) First digital cranial endocasts of late Oligocene Notohippidae (Notoungulata): implications for endemic South American ungulates brain evolution. J Mammal Evol 23(1):1–16

Edinger T (1950) Frontal sinus evolution (particularly in the Equidae). Bull Mus Comp Zool Harvard 103:411–496

Elliot-Smith GE (1898) The brain in the Edentata. Trans Linn Soc Lond Ser 2 (Zoology) 7:277–394

Engelmann GF (1985) The phylogeny of the Xenarthra. In: Montgomery GG (ed) The Evolution and Ecology of Armadillos, Sloths and Vermilinguas. Smithsonian Institution Press, Washington, D.C., pp 51–64

Esteban GI (1996) Revisión de los Mylodontinae cuaternarios (Edentata-Tardigrada) de Argentina, Bolivia y Uruguay. Sistemática, filogenia, paleobiología, paleozoogeografía y paleoecología. Dissertation, Universidad Nacional de Tucumán

Evans HE (1993) Miller's Anatomy of the Dog, 3rd edition. Saunders, Philadelphia

Fariña RA, Vizcaíno SF (2003) Slow moving or browsers? A note on nomenclature. Senckenb Biol 83(1):3–4

Farke AA (2007) Morphology, constraints, and scaling of frontal sinuses in the hartebeest, *Alcelaphus buselaphus* (Mammalia: Artiodactyla, Bovidae). J Morphol 268(3):243–253

Farke AA (2008) Function and evolution of the cranial sinuses in bovid mammals and ceratopsian dinosaurs. Dissertation, Stony Brook University

Farke AA (2010) Evolution and functional morphology of the frontal sinuses in Bovidae (Mammalia: Artiodactyla), and implications for the evolution of cranial pneumaticity. Zool J Linn Soc 159(4):988–1014

Fernicola JC, Toledo N, Bargo MS, Vizcaíno SF (2012) A neomorphic ossification of the nasal cartilages and the structure of paranasal sinus system of the glyptodont *Neosclerocalyptus* Paula Couto 1957 (Mammalia, Xenarthra). Palaeontol Electron 15(3):1–22

Fernicola JC, Vizcaíno SF, De Iuliis G (2009) The fossil mammals collected by Charles Darwin in South America during his travels on board the HMS Beagle. Rev Asoc Geol Argent 64(1):147–159

Flower W (1883) On the arrangement of the orders and families of existing Mammalia. Proc Zool Soc Lond 1883:178–186

Gaudin TJ (1995) The ear region of edentates and the phylogeny of the Tardigrada (Mammalia, Xenarthra). J Vertebr Paleontol 15(3):672–705

Gaudin TJ (2004) Phylogenetic relationships among sloths (Mammalia, Xenarthra, Tardigrada): the craniodental evidence. Zool J Linn Soc 140(2):255–305

Gaudin TJ, Croft DA (2015) Paleogene Xenarthra and the evolution of South American mammals. J Mammal 96(4):622–634

Gaudin TJ, De Iuliis G, Toledo N, Pujos F (2015) The basicranium and orbital region of the early Miocene *Eucholoeops ingens* Ameghino, (Xenarthra, Pilosa, Megalonychidae). Ameghiniana 52(2):226–240

Gelfo JN, Reguero MA, López GM, Carlini AA, Ciancio MR, Chornogubsky L, Bond M, Goin FJ, Tejedor M (2009) Eocene mammals and continental strata from Patagonia and Antarctic Peninsula. In: Albright LB (ed) Papers on Geology, Vertebrate Paleontology, and Biostratigraphy in Honor of Michael O. Woodburne. Mus North Ariz Bull 64, Flagstaff, Arizona, pp 567–592

Gervais P (1869) Mémoire sur les formes cérébrales propres aux édentés vivants et fossiles. Nouv Arch du Mus Hist Nat Paris 5:1–56

Gill T (1872) Arrangement of the families of mammals, with analytical tables. Smithson Misc Collect 11:1–98

Goffart M (1971) Function and Form in the Sloth. Pergamon Press, Oxford

Guth C (1961) La région temporale des Edentés. Dissertation, Université de Paris

Hayssen V (2008) *Bradypus pygmaeus* (Pilosa: Bradypodidae). Mammal Species 812:1–4

Hayssen V (2010) *Bradypus variegatus* (Pilosa: Bradypodidae). Mammal Species 42(850):19–32

Hoffstetter R (1952) Les mammifères Pléistocènes de La République de l'Equateur. Mem Soc Geol France 66:1–391

Hyrtl J (1854) Beiträge zur vergleichenden Angiologie. V. Das arterielle Gefäss-System der Edentaten. Denksch Akad Wiss Wien Math-Naturwiss Kl 6: 21–64.

Jerison HJ (1991) Fossil Brains and the evolution of the neocortex. In: Finlay BL, Innocenti G, Scheich H (eds) The Neocortex, Ontogeny and Phylogeny. Springer, Boston, pp 5–19

Kielan-Jaworowska Z (1986) Brain evolution in Mesozoic mammals. In: Flanagan KM, Lillegraven JA (eds) Vertebrates, Phylogeny, and Philosophy. Contrib Geol Univ Wyoming Spec Pap 3:21–34

Kraglievich L (1925) Cuatro nuevos Gravigrados de la fauna araucana chapadmalense. Anales Mus Nac Hist Nat Bernardino Rivadavia 33:215–235

Langworthy OR (1935) A physiological study of the cerebral motor cortex and the control of posture in the sloth. J Comp Neurol 62(2): 333–348

Macrini TE, Muizon C de, Cifelli RL, Rowe T (2007a) Digital cranial endocast of *Pucadelphys andinus*, a Paleocene metatherian. J Vertebr Paleontol 27(1):99–107

Macrini TE, Rougier GW, Rowe T (2007b) Description of a cranial endocast from the fossil mammal *Vincelestes neuquenianus* (Theriiformes) and its relevance to the evolution of endocranial characters in therians. Anat Rec 290(7):875–892

MacPhee RDE, Iturralde-Vinent MA (1994) First Tertiary land mammal from Greater Antilles: an early Miocene sloth (Xenarthra, Megalonychidae) from Cuba. Am Mus Novitates 3094:1–13

MacPhee RDE, Iturralde-Vinent MA (1995) Origin of the Greater Antillean land mammal fauna, 1: new Tertiary fossils from Cuba and Puerto Rico. Am Mus Novitates 3141:1–31

McAfee RK (2009) Reassessment of the cranial characters of *Glossotherium* and *Paramylodon* (Mammalia: Xenarthra: Mylodontidae). Zool J Linn Soc 155(4):885–903

McDonald HG, De Iuliis G (2008) Fossil history of sloths. In: Vizcaíno SF, Loughry WJ (eds) The Biology of the Xenarthra. University Press of Florida, Gainesville, pp 39–55

McDonald HG, Rincón AD, Gaudin TJ (2013) A new genus of megalonychid sloth (Mammalia, Xenarthra) from the late Pleistocene (Lujanian) of Sierra De Perija, Zulia State, Venezuela. J Vertebr Paleontol 33(5):1226–1238

McKenna MC, Bell SK (1997) Classification of Mammals Above the Species Level. Columbia University Press, New York

Mones A (1986) Palaeovertebrata Sudamericana. Catálogo sistemático de los vertebrados fósiles de América del Sur. Parte I. Lista preliminar y bibliografía. Cour Forsch Inst Senckenberg 82:1–625

Moore WJ (1981) The Mammalian Skull. Cambridge University Press, Cambridge

Naples VL (1982) Cranial osteology and function in the tree sloths, *Bradypus* and *Choloepus*. Am Mus Novitates 2739:1–41

Novacek MJ (1993) Patterns of diversity in the mammalian skull. In: Hanken J, Hall BK (eds) The Skull, Volume 2, Patterns of Structural and Systematic Diversity. University of Chicago Press, Chicago, pp 438–545

Owen R (1839) Fossil Mammalia. In: Darwin C (ed) The Zoology of the Voyage of the Beagle. Smith, Elder and Co., London, pp 13–111

Owen R (1842) Description of the skeleton of an extinct gigantic sloth, *Mylodon robustus*, Owen, with observations on the osteology, natural affinities, and probable habits of the megatheroid quadrupeds in general. Direction of the Council, London

Pascual R (2006) Evolution and geography: the biogeographic history of South American land mammals. Ann Mo Bot Gard 93:209–230

Patterson B, Turnbull WD, Segall W, Gaudin TJ (1992) The ear region in xenarthrans (= Edentata: Mammalia). Part II. Pilosa (sloths, anteaters), palaeanodonts, and a miscellany. Fieldiana Geol 24:1–78

Pérez LM, Toledo N, De Iuliis G, Bargo MS, Vizcaíno SF (2010) Morphology and function of the hyoid apparatus of fossil xenarthrans (Mammalia). J Morphol 271:1119–1133

Pitana VG, Esteban GI, Ribeiro AM, Cartelle C (2013) Cranial and dental studies of *Glossotherium robustum* (Owen, 1842) (Xenarthra: Pilosa: Mylodontidae) from the Pleistocene of southern Brazil. Alcheringa 37(2):147–162

Prothero JW, Sundsten JW (1984) Folding of the cerebral cortex in mammals. Brain Behav Evol 24(2-3):152–167

Pujos F, De Iuliis G, Cartelle C (2017) A paleogeographic overview of tropical fossil sloths: towards an understanding of the origin of extant suspensory sloths? J Mammal Evol 24(1):1–20

Pujos F, Gaudin TJ, De Iuliis G, Cartelle C (2012) Recent advances on variability, morpho-functional adaptations, dental terminology, and evolution of sloths. J Mammal Evol 19(3):159–169

Reguero MA, Gelfo JN, López GM, Bond M, Abello A, Santillana SN, Marenssi SA (2014) Final Gondwana breakup: the Paleogene South American native ungulates and the demise of the South America–Antarctica land connection. Glob Planet Change 123:400–413

Roth G, Dicke U (2005) Evolution of the brain and intelligence. Trends Cogn Sci 9(5):250–257

Sakai ST, Arsznov BM, Lundrigan BL, Holekamp KE (2011) Brain size and social complexity: a computed tomography study in Hyaenidae. Brain Behav Evol 77(2):91–104

Simpson GG (1980) Splendid Isolation. The Curious History of South American Mammals. Yale University Press, New Haven

Simpson GG, Paula Couto C de (1981) Fossil mammals from the Cenozoic of Acre, Brazil. III - Pleistocene Edentata Pilosa, Proboscidea, Sirenia, Perissodactyla and Artiodactyla. Iheringia Ser Geol 6:11–73

Slater GJ, Cui P, Forasiepi AM, Lenz D, Tsangaras K, Voirin B, de Moraes-Barros N, MacPhee RDE, Greenwood AD (2016) Evolutionary relationships among extinct and extant sloths: the evidence of mitogenomes and retroviruses. Genome Biol Evol 8(3): 607–621

St-André PA, Pujos F, Cartelle C, De Iuliis G, Gaudin TJ, McDonald HG, Quispe BM (2010) Nouveaux paresseux terrestres (Mammalia, Xenarthra, Mylodontidae) du Néogène de l'Altiplano bolivien. Geodiversitas 32(2):255–306

Storch G, Habersetzer J (1991) Rückverlagerte Choanen und akzessorische Bulla tympanica bei rezenten Vermilingua und *Eurotamandua* aus dem Eozän von Messel (Mammalia: Xenarthra). Z Säugetierk 56:257–271

Tandler J (1901) Zur vergleichenden Anatomie der Kopfarterien bei den Mammalia. Anat Hefte 18: 328–368.

Thiery G, Ducrocq S (2015) Endocasts and brain evolution in Anthracotheriidae (Artiodactyla, Hippopotamoidea). J Anat 227(3):277–285

Van der Merwe NJ, Bezuidenhout AJ, Seegers CD (1995) The skull and mandible of the African elephant (*Loxodonta africana*). Onderstepoort J Vet Res 62(4):245–260

Varela L, Fariña RA (2016) Co-occurrence of mylodontid sloths and insights on their potential distributions during the late Pleistocene. Quaternary Res 85(1):66–74

Vinuesa V, Iurino DA, Madurell-Malapeira J, Liu J, Fortuny J, Sardella R, Alba DM (2016) Inferences of social behavior in bone-cracking hyaenids (Carnivora, Hyaenidae) based on digital paleoneurological techniques: implications for human–carnivoran interactions in the Pleistocene. Quaternary Internatl 413:7–14

Vizcaíno SF, Zárate M, Bargo MS, Dondas A (2001) Pleistocene burrows in the Mar del Plata area (Argentina) and their probable builders. Acta Palaeontol Pol 46(2):289–301

Weidenreich F (1924) Über die pneumatischen Nebenräume des Kopfes. Ein Beitrag zur Kenntnis des Bauprinzips der Knochen, des Schädels und des Körpers (Knochenstudien: III. Teil). Anat Embryol 72(1):55–93

Weidenreich F (1941) The brain and its role in the phylogenetic transformation of the human skull. Trans Am Phil Soc 31(5): 320–442

Wible JR (2010) Petrosal anatomy of the nine-banded armadillo, *Dasypus novemcinctus* Linnaeus, 1758 (Mammalia, Xenarthra, Dasypodidae). Ann Carnegie Mus 79(1):1–28

Witmer LM (1997) The evolution of the antorbital cavity of archosaurs: a study in soft-tissue reconstruction in the fossil record with an analysis of the function of pneumaticity. J Vertebr Paleontol 17(S1):1–73

Woodburne MO (2010) The Great American Biotic Interchange: dispersals, tectonics, climate, sea level and holding pens. J Mammal Evol 17(4):245–264